

## [Supporting Information]

### **Self-assembly of D-penicillaminato $M_6M'_8$ ( $M = Ni^{II}, Pd^{II}, Pt^{II}$ ; $M' = Cu^I, Ag^I$ ) clusters and their organization into extended $La^{III}M_6M'_8$ supramolecular structures**

**Nobuto Yoshinari and Takumi Konno\***

Department of Chemistry, Graduate School of Science, Osaka University, Toyonaka, Osaka  
560-0043, Japan.

\* To whom correspondence should be addressed.

E-mail: konno@chem.sci.osaka-u.ac.jp

## X-Ray structure determination

Single-crystal X-ray diffraction experiments for  $\text{La}_2[\mathbf{1}](\text{CH}_3\text{COO})$  was performed on a Bruker SMART APEX diffractometer with a graphite-monochromated Mo-K $\alpha$  radiation. The intensity data were collected by the  $\omega$ - $2\theta$  scan mode. The data integration and reduction were undertaken with SAINT and XPREP. An empirical absorption correction with SADABS was applied to each data set. Single-crystal X-ray diffraction measurements for  $\text{La}_2[\mathbf{2}](\text{CH}_3\text{COO})$ ,  $\text{La}_2[\mathbf{3}](\text{CH}_3\text{COO})$ ,  $\text{La}_2[\mathbf{4}](\text{CH}_3\text{COO})$ ,  $\text{La}_2[\mathbf{5}](\text{CH}_3\text{COO})$ ,  $\text{La}_2[\mathbf{6}]\text{Cl}$  and  $\text{La}_2[\mathbf{6}]\text{Cl}\cdot\text{HCl}$  were made on a Rigaku RAXIS-RAPID imaging plate area detector with a graphite monochromated Mo-K $\alpha$  radiation. The intensity data were collected by the  $\omega$  scan technique and were empirically corrected for absorption. The structures were solved by direct methods and were refined with full-matrix least-squares on  $F^2$ . Hydrogen atoms except those of water molecules were placed at calculated positions but were not refined. All calculations were performed using Yadokari-XG 2009 software package,<sup>15</sup> except the refinements that were performed using SHELXL-97.<sup>16</sup>

For  $\text{La}_2[\mathbf{1}](\text{CH}_3\text{COO})$ , a La atom was disordered in four positions (La2–La5). All non-hydrogen atoms except solvated water molecules, disordered La atoms and O36 of an aqua ligand that bound to La2 were refined anisotropically. ISOR restraints were used for several carbon and oxygen atoms in the complex anion. For  $\text{La}_2[\mathbf{2}](\text{CH}_3\text{COO})$ , one La atom was disordered in three positions (La2–La4). All non-hydrogen atoms except solvated water molecules and disordered atoms were refined anisotropically. ISOR restraints were used for several carbon and oxygen atoms in the complex anion. A SIMU restraint was applied for an acetate anion (C61/C62/O27/O28). For  $\text{La}_2[\mathbf{3}](\text{CH}_3\text{COO})$ , one La atom was disordered in six positions (La2–La7). One of carboxylate groups (C18/O7/O8) was disordered in two positions, which were treated with DFIX and SIMU restraints. All non-hydrogen atoms except solvated water molecules and disordered atoms were refined anisotropically. DFIX restraints were used for two carboxylate groups (C13/O5/O6, C58/O23/O24). A SIMU restraint was used for an acetate anion (C61/C62/O27/O28). DFIX restraints were used for some solvated water molecules in order to avoid unusual O...O distances. For  $\text{La}_2[\mathbf{4}](\text{CH}_3\text{COO})$ , one La atom was disordered in three positions (La2A, La3A, La3B). Each of two carboxylate groups (C23/O9/O10, C43/O17/O18) was disordered into two positions, which were treated with

DFIX and EADP restraints. All non-hydrogen atoms except solvated water molecules and disordered atoms were refined anisotropically. For  $\text{La}_2[\mathbf{5}](\text{CH}_3\text{COO})$ , one La atom was disordered in six positions (La2–La7). DFIX and SIMU restraints were used for two carboxylate groups (C18/O7/O8, C58/O23/O24). A SIMU restraint was used for an acetate anion (C61/C62/O27/O28). DFIX restraints were used for some solvated water molecules in order to avoid unusual O...O distances. For  $\text{La}_2[\mathbf{6}]\text{Cl}$ , a chloride anion (Cl2) and one of solvated water molecules (O13) were disordered and occupied the same position, which were treated with EADP and EXYZ restraints. Oxygen atoms that bound to La2 (O5/O6/O11/O12) were disordered. All non-hydrogen atoms except disordered atoms were refined anisotropically. For  $\text{La}_2[\mathbf{6}]\text{Cl}\cdot\text{HCl}$ , A carboxyl group (C58/O23/O24/H110) was disordered in two positions. All non-hydrogen atoms except disordered atoms and solvated water molecules were refined anisotropically. ISOR restraints were used for several carbon and oxygen atoms in the complex anion. DFIX restraints were used for some solvated water molecules in order to avoid unusual O...O distances.

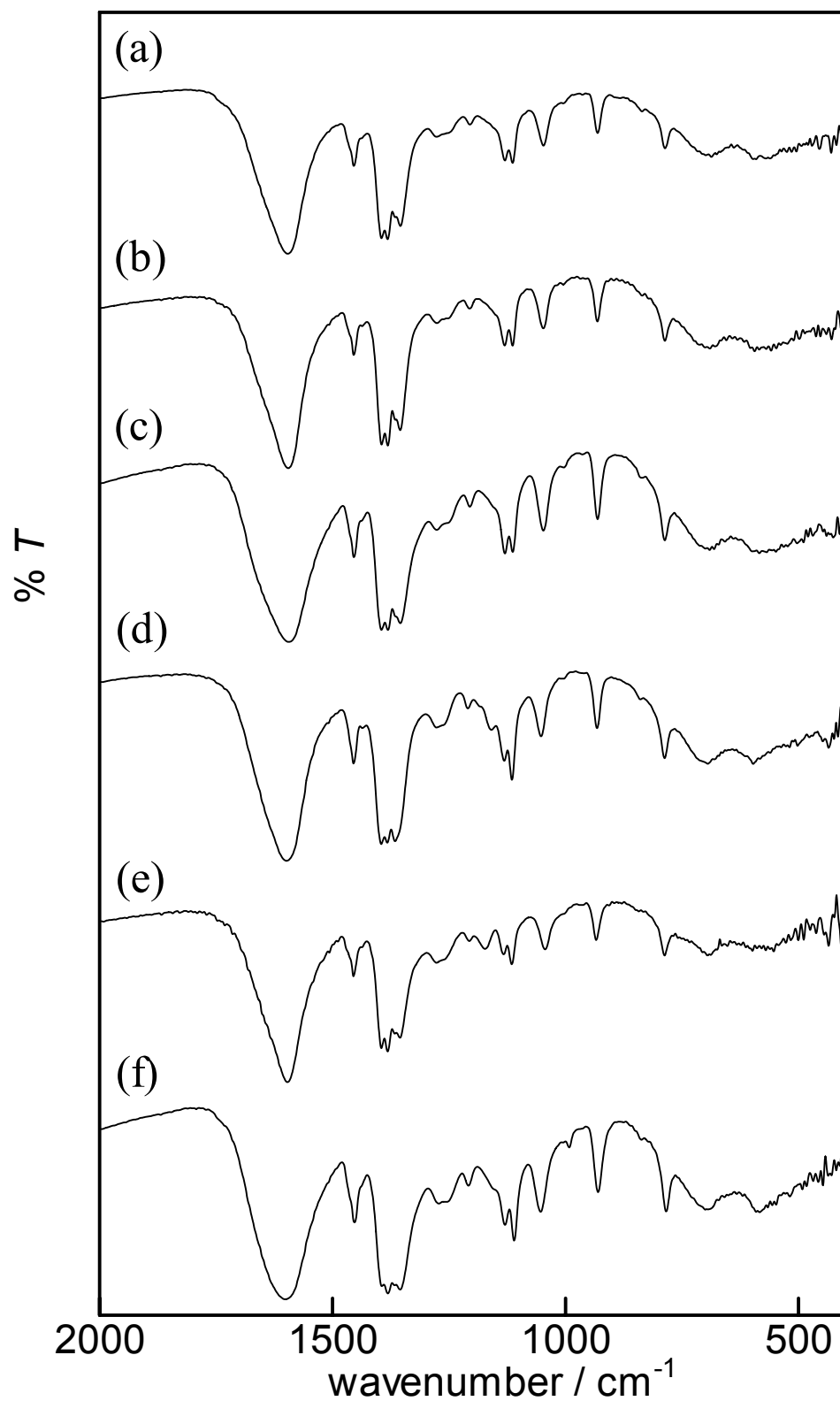


**Figure S1** IR spectra (KBr pellet) of (a) Na<sub>5</sub>[**1**], (b) Na<sub>5</sub>[**2**], (c) Na<sub>5</sub>[**3**], (d) K<sub>5</sub>[**4**], (e) K<sub>5</sub>[**5**] and (f) Na<sub>5</sub>[**6**].

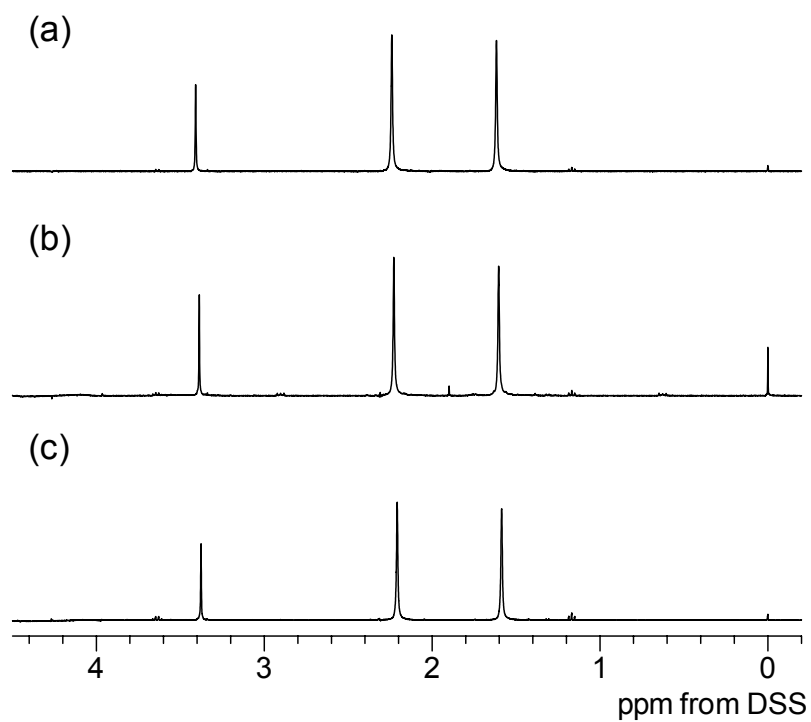


**Figure S2**  $^1\text{H}$  NMR spectra of (a)  $\text{Na}_5[\mathbf{1}]$ , (b)  $\text{Na}_5[\mathbf{2}]$  and (c)  $\text{Na}_5[\mathbf{3}]$  in  $\text{D}_2\text{O}$ .

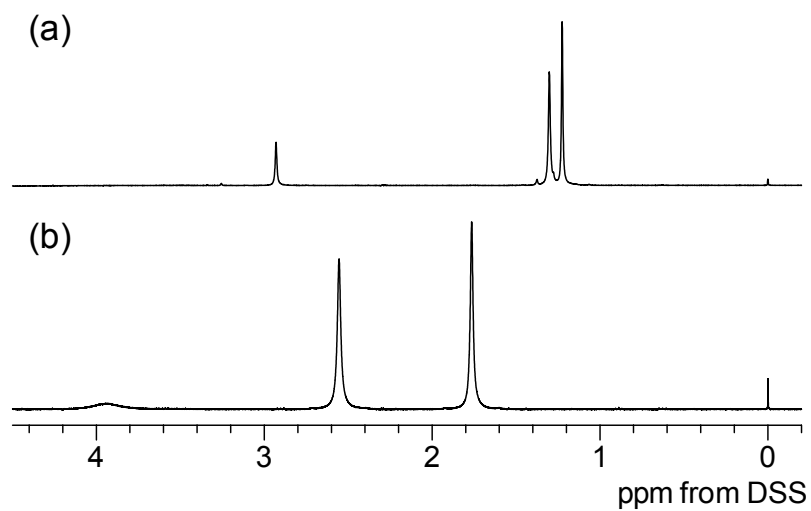


**Figure S3**  $^1\text{H}$  NMR spectra of (a) *cis*- $\text{K}_2[\text{Ni}(\text{D-pen-}N,S)_2]$  and (b)  $\text{K}_5[\mathbf{4}]$  in  $\text{D}_2\text{O}$ .

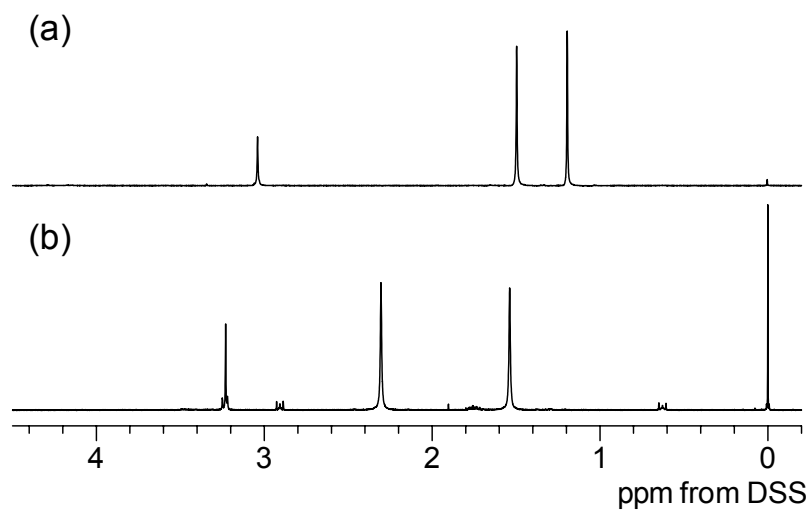


**Figure S4** <sup>1</sup>H NMR spectra of (a) *cis*-K<sub>2</sub>[Pt(D-pen-*N,S*)<sub>2</sub>] and (b) K<sub>5</sub>[**5**] in D<sub>2</sub>O.

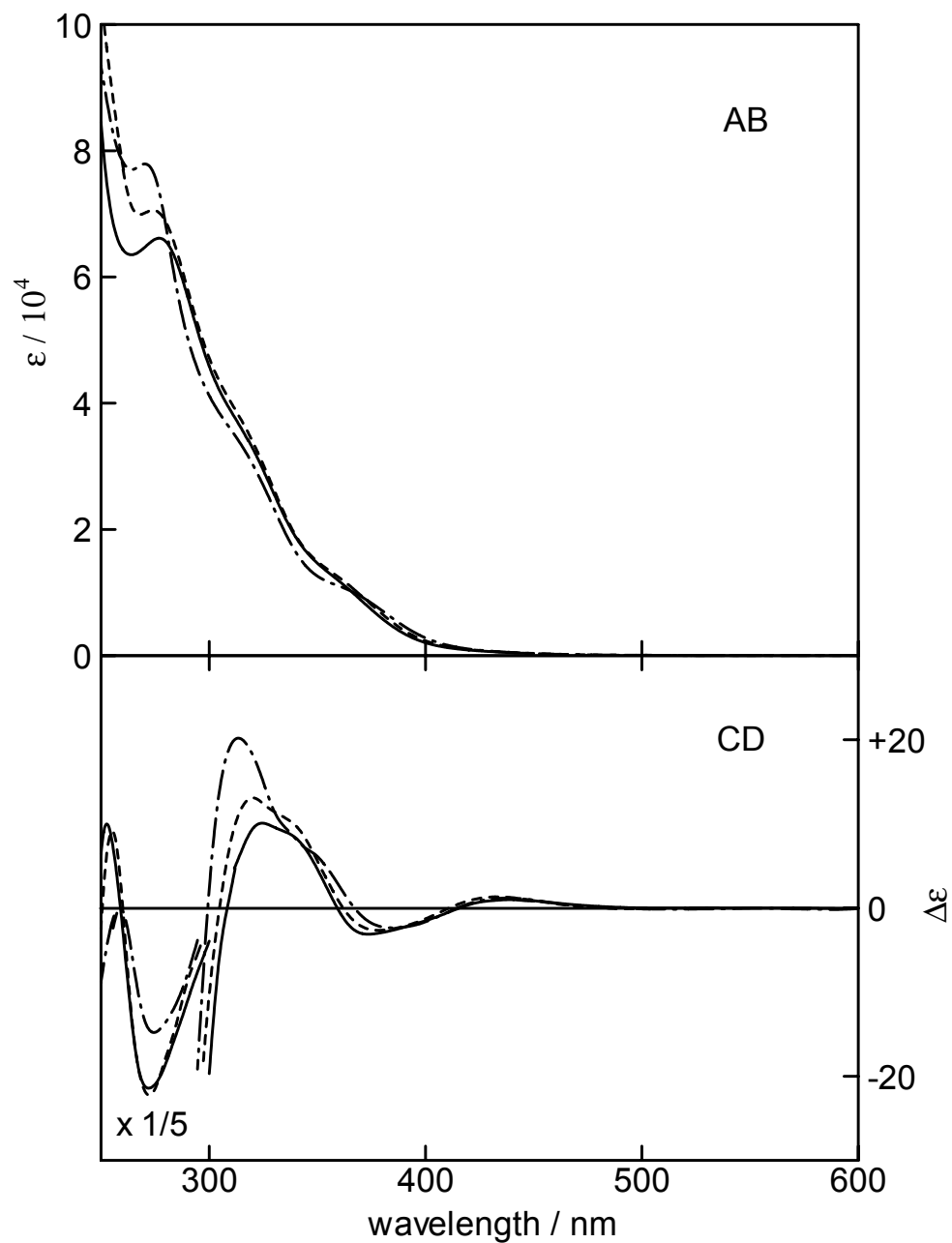


**Figure S5** Electronic absorption and CD spectra of Na<sub>5</sub>[1] (—), Na<sub>5</sub>[2] (---) and Na<sub>5</sub>[3] (---) in H<sub>2</sub>O.

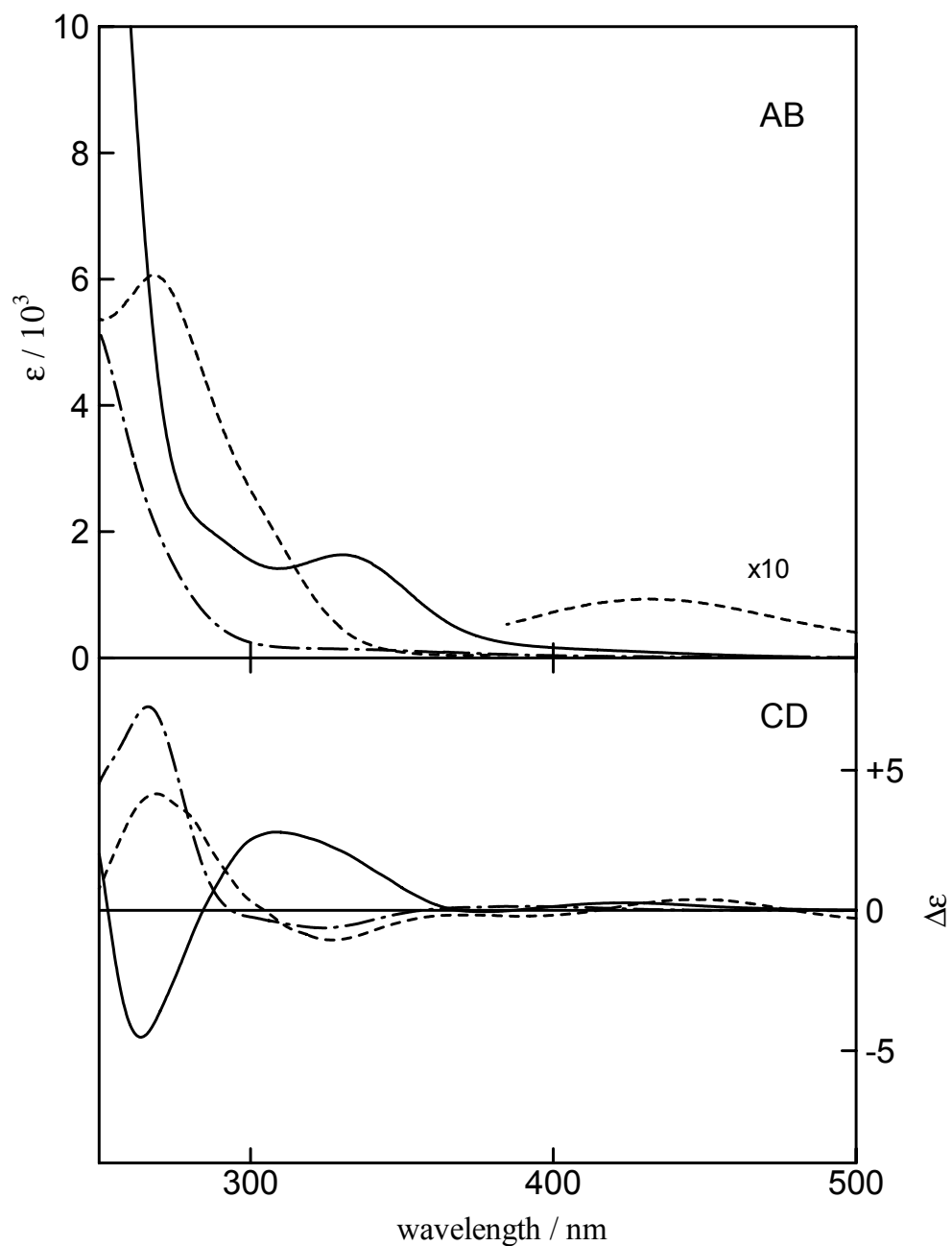


**Figure S6** Electronic absorption and CD spectra of *cis*-Na<sub>2</sub>[Pd(D-pen-*N,S*)<sub>2</sub>] (—), *cis*-K<sub>2</sub>[Ni(D-pen-*N,S*)<sub>2</sub>] (---) and *cis*-K<sub>2</sub>[Pt(D-pen-*N,S*)<sub>2</sub>] (-·-) in H<sub>2</sub>O.



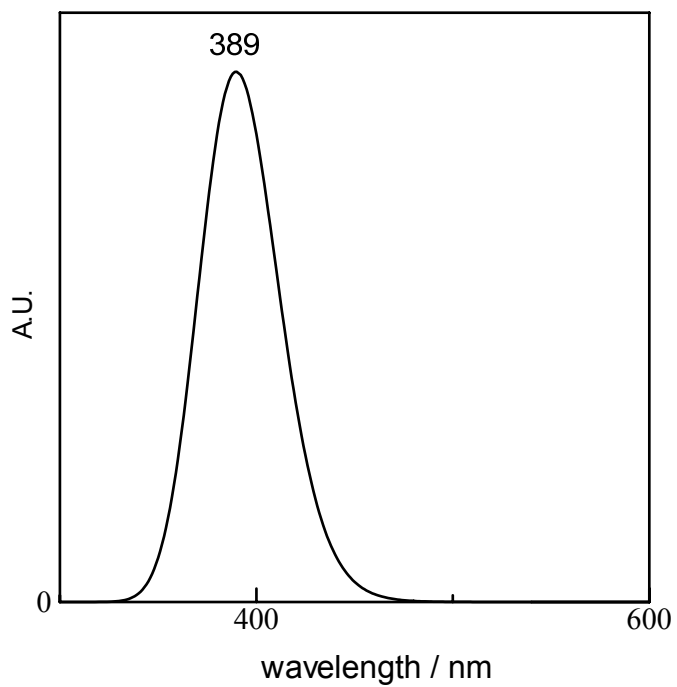


**Figure S7** A simulated electronic absorption spectrum for  $[6']^{7+}$ .

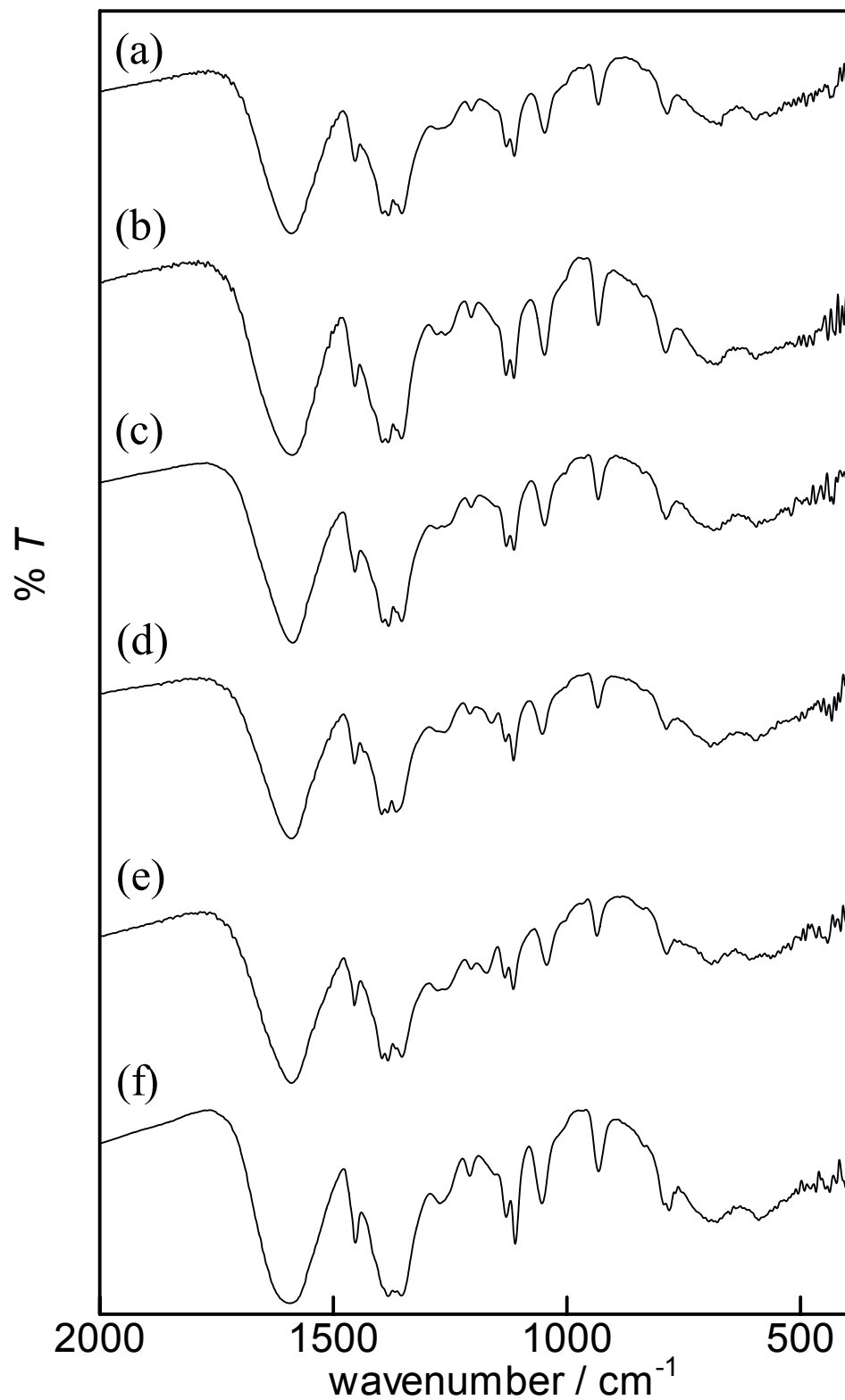


**Figure S8** IR spectra (KBr pellet) of (a)  $\text{La}_2[\mathbf{1}](\text{CH}_3\text{COO})$ , (b)  $\text{La}_2[\mathbf{2}](\text{CH}_3\text{COO})$ , (c)  $\text{La}_2[\mathbf{3}](\text{CH}_3\text{COO})$ , (d)  $\text{La}_2[\mathbf{4}](\text{CH}_3\text{COO})$ , (e)  $\text{La}_2[\mathbf{5}](\text{CH}_3\text{COO})$  and (f)  $\text{La}_2[\mathbf{6}]\text{Cl}$ .

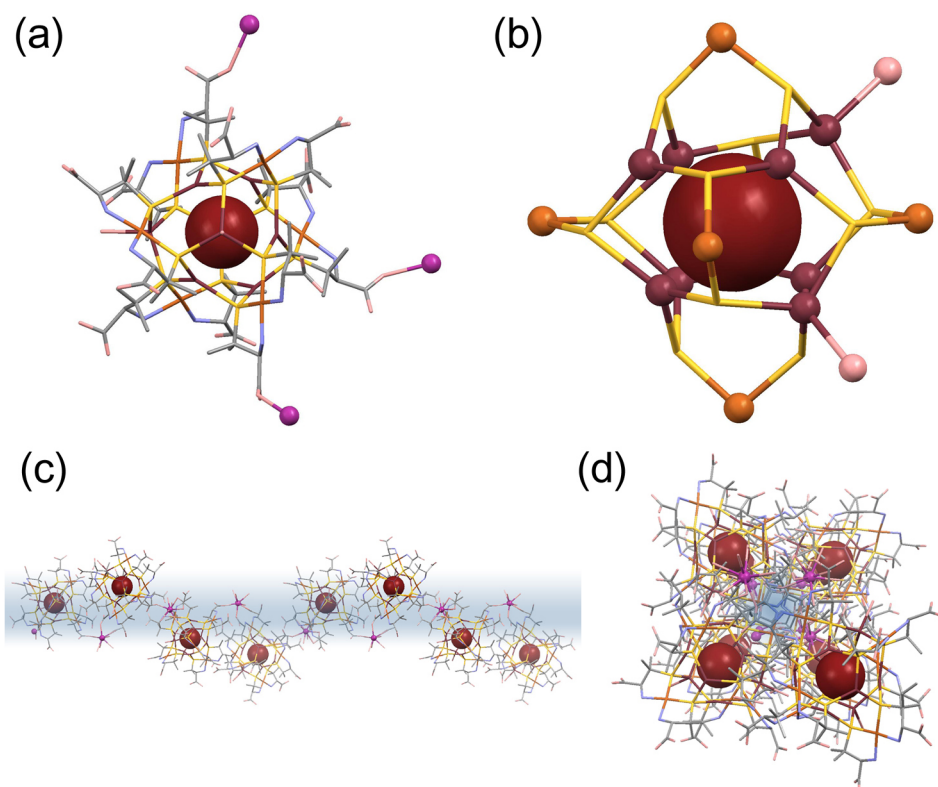


**Figure S9** Perspective views of (a) the  $\text{Pd}^{\text{II}}_6\text{Ag}^{\text{I}}_8\text{Br}$  cluster-unit bound to  $\text{La}^{3+}$  ions, (b) the core structure of the  $\text{Pd}^{\text{II}}_6\text{Ag}^{\text{I}}_8\text{Br}$  cluster-unit, (c) the 1D helix structure looking down  $b$ -axis and (d) the 1D helix structure looking down  $c$ -axis in  $\text{La}_2[2](\text{CH}_3\text{COO})$ . H atoms are omitted for clarity. La: purple, Pd: orange, Ag: red purple, Br: brown, C: gray, N: blue, O: red, S: yellow.

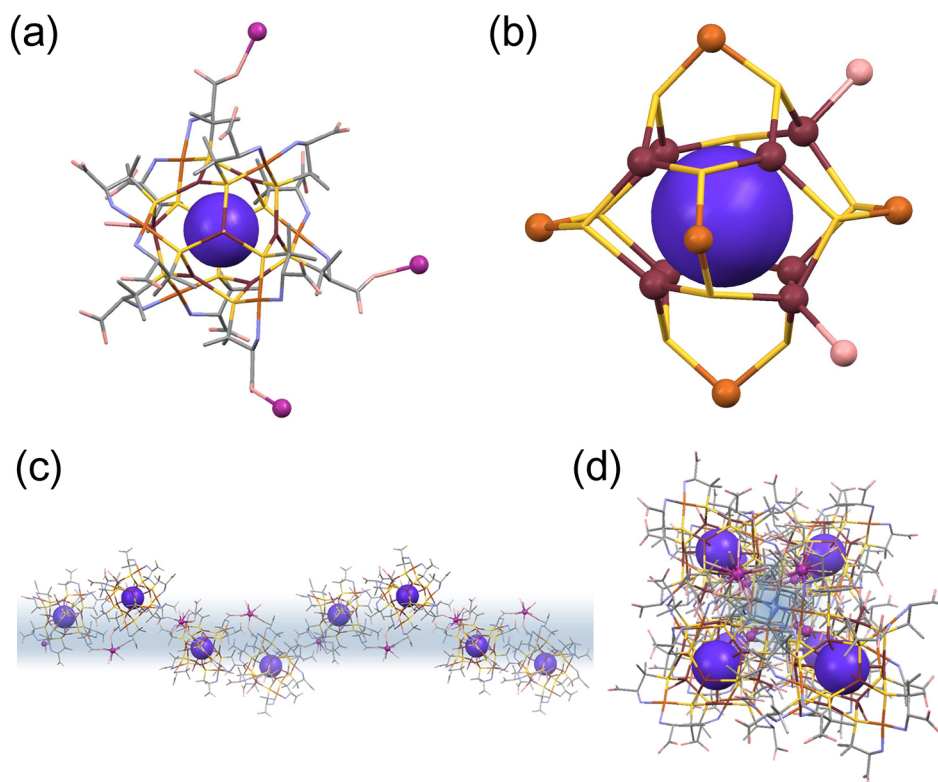


**Figure S10** Perspective views of (a) the  $\text{Pd}^{\text{II}}_6\text{Ag}^{\text{I}}_8\text{I}$  cluster-unit bound to  $\text{La}^{3+}$  ions, (b) the core structure of the  $\text{Pd}^{\text{II}}_6\text{Ag}^{\text{I}}_8\text{I}$  cluster-unit, (c) the 1D helix structure looking down  $b$ -axis and (d) the 1D helix structure looking down  $c$ -axis in  $\text{La}_2[\mathbf{3}](\text{CH}_3\text{COO})$ . H atoms are omitted for clarity. La: purple, Pd: orange, Ag: red purple, I: deep purple, C: gray, N: blue, O: red, S: yellow.

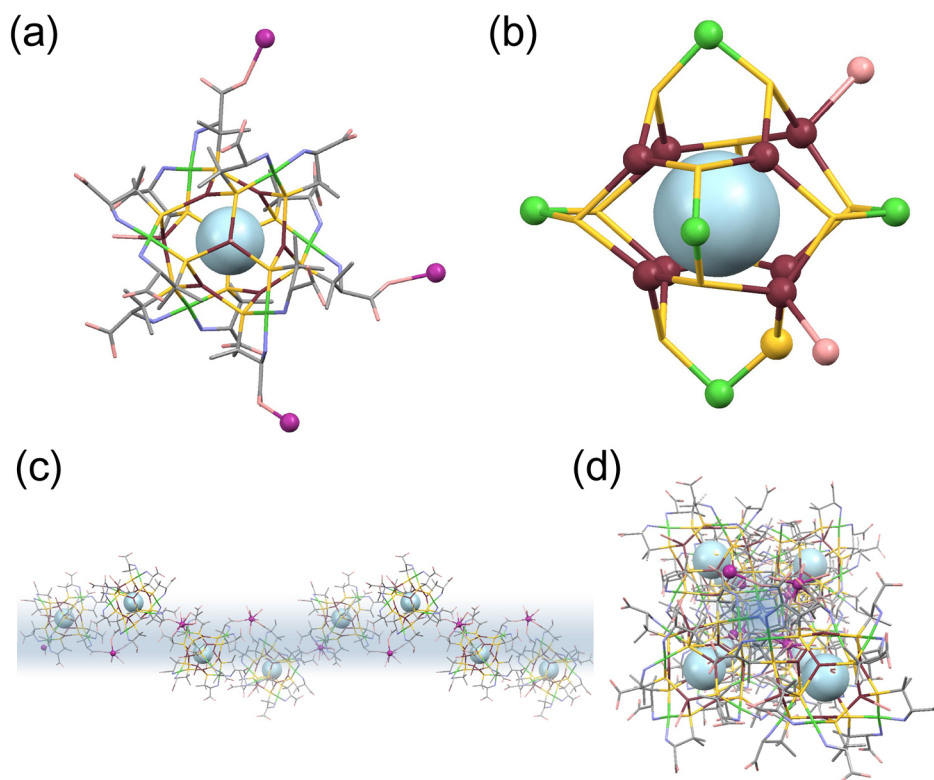


**Figure S11** Perspective views of (a) the Ni<sup>II</sup><sub>6</sub>Ag<sup>I</sup><sub>8</sub>Cl cluster-unit bound to La<sup>3+</sup> ions, (b) the core structure of the Ni<sup>II</sup><sub>6</sub>Ag<sup>I</sup><sub>8</sub>Cl cluster-unit, (c) the 1D helix structure looking down *b*-axis and (d) the 1D helix structure looking down *c*-axis in La<sub>2</sub>[4](CH<sub>3</sub>COO). H atoms are omitted for clarity. La: purple, Ni: light green, Ag: red purple, Cl: pale blue, C: gray, N: blue, O: red, S: yellow.

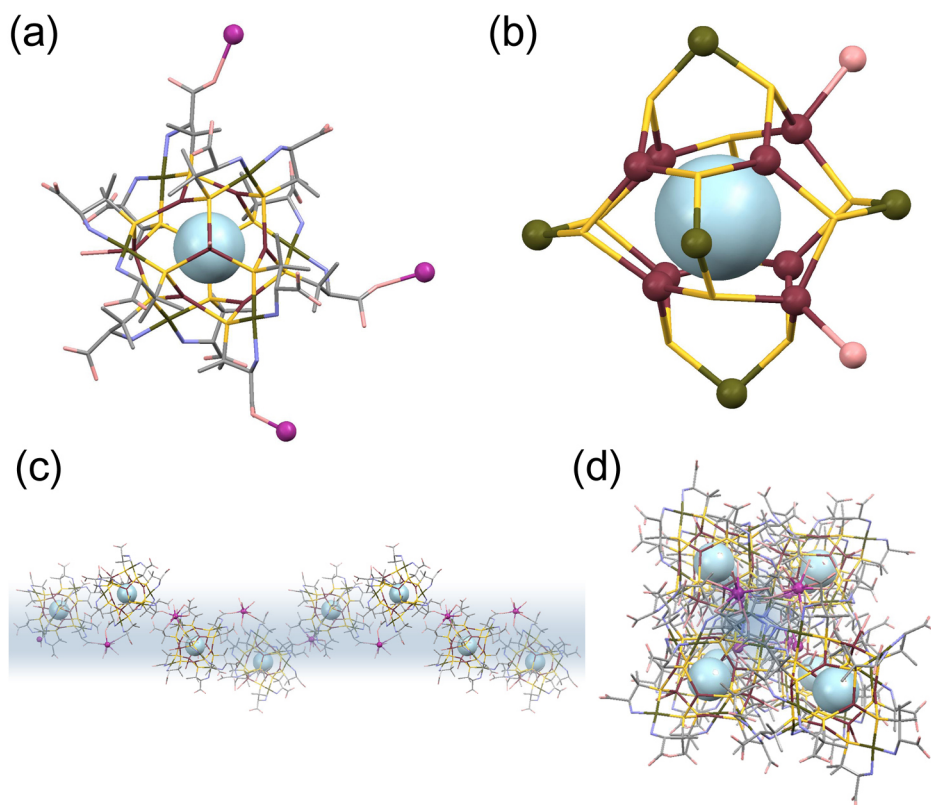


**Figure S12** Perspective views of (a) the Pt<sup>II</sup><sub>6</sub>Ag<sup>I</sup><sub>8</sub>Cl cluster-unit bound to La<sup>3+</sup> ions, (b) the core structure of the Pt<sup>II</sup><sub>6</sub>Ag<sup>I</sup><sub>8</sub>Cl cluster-unit, (c) the 1D helix structure looking down *b*-axis and (d) the 1D helix structure looking down *c*-axis in La<sub>2</sub>[**5**](CH<sub>3</sub>COO). H atoms are omitted for clarity. La: purple, Pt: dark yellow, Ag: red purple, Cl: pale blue, C: gray, N: blue, O: red, S: yellow.

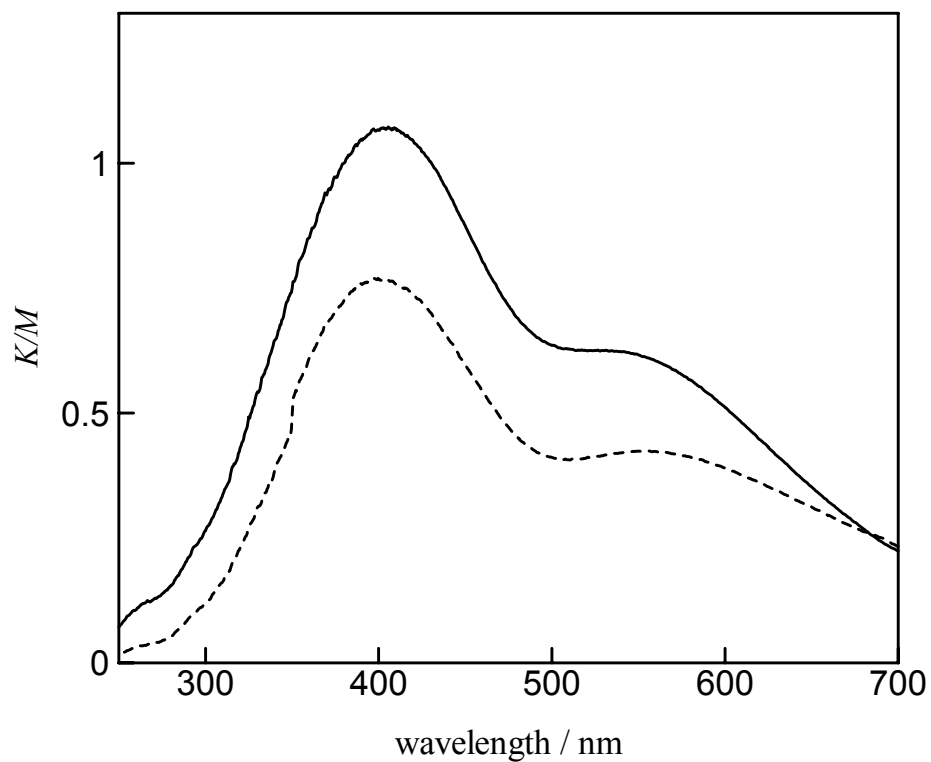


**Figure S13** Diffuse reflection spectra of  $\text{La}_2[\mathbf{6}]\text{Cl}$  (—) and  $\text{La}_2[\mathbf{6}]\text{Cl}\cdot\text{HCl}$  (---).

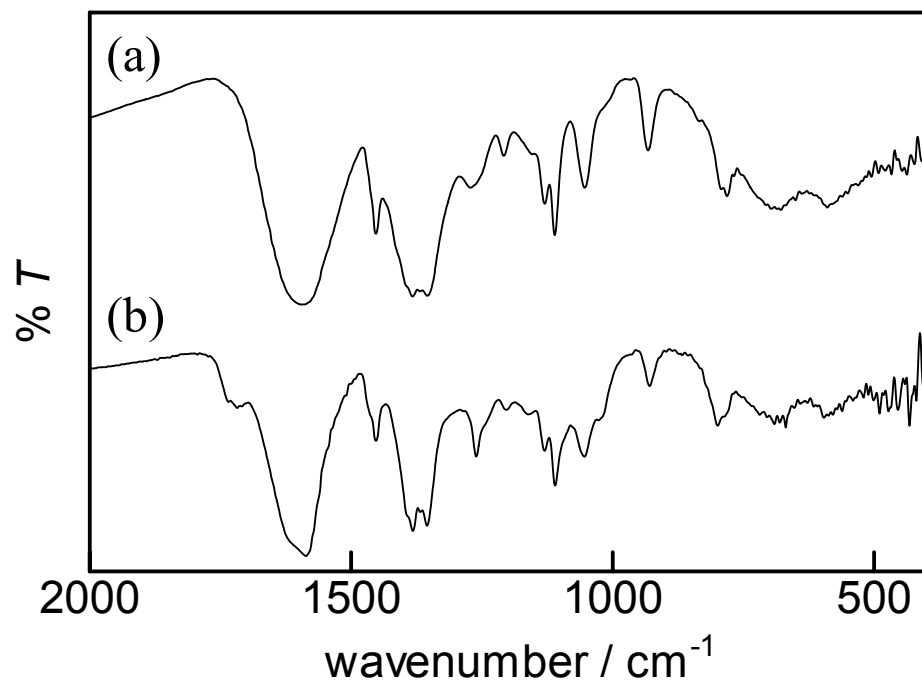


**Figure S14** IR spectra (KBr pellet) of (a)  $\text{La}_2[\mathbf{6}]\text{Cl}$  and (b)  $\text{La}_2[\mathbf{6}]\text{Cl}\cdot\text{HCl}$ .

**Table S1** Mulliken polulation of MOs near frontier orbitals for [6']<sup>7+</sup>.

Orbital	Energy / eV	Pd	Cu	SH	Cl	NH <sub>3</sub>
L+9	-15.22	0.02	0.61	0.23	0.01	0.13
L+8	-15.22	0.02	0.61	0.23	0.01	0.13
L+7	-15.59	0.12	0.75	0.13	0.00	0.01
L+6	-16.03	0.00	0.60	0.32	0.00	0.09
L+5	-17.38	0.43	0.05	0.30	0.00	0.23
L+4	-17.38	0.43	0.05	0.30	0.00	0.23
L+3	-17.38	0.43	0.05	0.30	0.00	0.23
L+2	-17.48	0.43	0.07	0.28	0.00	0.23
L+1	-17.48	0.43	0.07	0.28	0.00	0.23
LUMO	-17.48	0.43	0.07	0.28	0.00	0.23
HOMO	-21.49	0.15	0.41	0.43	0.00	0.00
H-1	-21.49	0.15	0.41	0.43	0.00	0.00
H-2	-21.57	0.15	0.43	0.37	0.02	0.02
H-3	-21.57	0.16	0.43	0.37	0.01	0.02
H-4	-21.57	0.16	0.43	0.38	0.01	0.03
H-5	-21.6	0.17	0.42	0.37	0.00	0.03
H-6	-21.63	0.15	0.44	0.37	0.01	0.02
H-7	-21.63	0.15	0.44	0.37	0.01	0.02
H-8	-21.91	0.21	0.50	0.27	0.00	0.01
H-9	-21.91	0.21	0.50	0.27	0.00	0.01
H-10	-22.15	0.08	0.61	0.14	0.16	0.01
H-11	-22.16	0.12	0.58	0.16	0.13	0.01
H-12	-22.16	0.12	0.58	0.16	0.13	0.01
H-13	-22.22	0.17	0.55	0.25	0.02	0.01
H-14	-22.25	0.15	0.58	0.22	0.04	0.01
H-15	-22.26	0.15	0.58	0.22	0.04	0.01
H-16	-22.35	0.83	0.05	0.08	0.00	0.04
H-17	-22.42	0.56	0.30	0.05	0.03	0.05
H-18	-22.42	0.56	0.30	0.05	0.03	0.05
H-19	-22.43	0.61	0.27	0.05	0.02	0.05
H-20	-22.61	0.68	0.17	0.04	0.00	0.10
H-21	-22.61	0.68	0.17	0.04	0.00	0.10
H-22	-22.63	0.30	0.56	0.13	0.00	0.01
H-23	-22.63	0.40	0.44	0.12	0.00	0.04
H-24	-22.63	0.41	0.43	0.12	0.00	0.04
H-25	-22.64	0.32	0.52	0.13	0.00	0.03
H-26	-22.81	0.16	0.76	0.06	0.00	0.01
H-27	-22.83	0.17	0.75	0.06	0.00	0.01
H-28	-22.84	0.17	0.75	0.06	0.00	0.01
H-29	-22.94	0.13	0.80	0.04	0.00	0.02



**Table S2** Energy, oscillator strength and major contribution of calculated transitions for  $[6^*]^{7+}$ .

Excited state	Energy /eV (/nm)	Oscillator strength	Major contributions <sup>a</sup>		
1.	2.97 (417)	0.0002	H-1->L+2	(0.27)	
2.	2.97 (417)	0.0004	H-1->L+2	(0.14)	
3.	2.97 (417)	0.0004	H-1->LUMO	(0.29)	
4.	3.01 (411)	0.0002	H-1->L+3	(0.10)	
5.	3.01 (411)	0.0002	H-1->L+4	(0.10)	
6.	3.01 (411)	0.0002	H-1->L+5	(0.38)	
7.	3.05 (406)	0.0000	H-7->L+2	(0.13)	
8.	3.06 (405)	0.0002	H-6->LUMO	(0.11)	
9.	3.06 (405)	0.0002	H-7->LUMO	(0.10)	
10.	3.09 (401)	0.0004	H-5->L+4	(0.10)	
11.	3.09 (401)	0.0005	H-5->L+3	(0.12)	
12.	3.10 (401)	0.0005	H-4->L+5	(0.14)	
13.	3.14 (394)	0.0020	H-9->L+4	(0.02)	
14.	3.14 (394)	0.0019	H-7->LUMO	(0.10)	
15.	3.14 (394)	0.0088	H-7->L+1	(0.10)	
16.	3.19 (388)	0.0137	H-26->L+4	(0.03),	H-9->LUMO (0.02),
			H-9->L+2	(0.03),	H-9->L+4 (0.02),
			H-8->LUMO	(0.03),	H-8->L+1 (0.03),
			H-7->L+4	(0.07),	H-6->L+3 (0.03),
			H-6->L+5	(0.02),	H-2->L+3 (0.08),
			H-1->L+1	(0.02),	H-1->L+4 (0.08),
			HOMO->L+2	(0.02)	
17.	3.19 (388)	0.0138	H-26->L+4	(0.03),	H-9->LUMO (0.04),
			H-9->L+1	(0.03),	H-8->L+2 (0.03),
			H-8->L+5	(0.02),	H-7->L+3 (0.03),
			H-6->L+5	(0.06),	H-2->L+4 (0.03),
			H-2->L+5	(0.05),	H-1->L+2 (0.02),
			HOMO->L+1	(0.02),	HOMO->L+5 (0.07)
18.	3.19 (388)	0.0171	H-26->L+3	(0.02)	H-9->L+1 (0.05),
			H-9->L+3	(0.04),	H-8->L+2 (0.04),
			H-7->L+3	(0.07),	H-6->L+4 (0.03),
			H-6->L+5	(0.04),	H-2->L+4 (0.07),
			H-2->L+5	(0.05),	H-1->L+3 (0.02)
19.	3.27 (379)	0.0017	HOMO->L+2	(0.10)	
20.	3.27 (379)	0.0018	HOMO->LUMO	(0.38)	

<sup>a</sup> for excited state 16-18, not only major contributions but also minor contributions are listed.